Blends of Metal Acetates and Polyurethanes Containing Pyridine Groups

CHANG ZHENG YANG,* XIAOMANG ZHANG, ELLEN M. O'CONNELL, RICHARD J. GODDARD, and S. L. COOPER†

Department of Chemical Engineering, University of Wisconsin-Madison, Madison, Wisconsin 53706-1695

SYNOPSIS

Two series of segmented polyurethanes based on 3/2/1 and 2/1/1 molar ratios of methylene diphenyldiisocyanate (MDI), *N,N*-bis(2-hydroxyethyl)isonicotinamide (BIN), and poly(tetramethylene oxide) (PTMO, MW = 1000) were synthesized and blended with different metal acetates. The thermal behavior and mechanical properties of the pyridine-containing polyurethane precursors and their blends were characterized by DSC, DMTA, and tensile testing. The results suggest that coordination between pyridine groups in the hard segments and the metal ions in the acetates improves hard-domain cohesion and phase separation and, subsequently, has an effect on mechanical properties. The varying ability of the pyridine group to coordinate with different cations results in different extents of phase separation. The interaction of pyridine with Ni or Cu(II) is much stronger than with Zn. It is shown that coordination interactions can be a driving force for phase separation and hard-domain aggregation in multiblock copolymer systems. Two different morphologies are proposed for polyurethanes of differing stoichiometry to explain the differences in the results from DMTA and tensile testing. © 1994 John Wiley & Sons, Inc.

INTRODUCTION

Thermoplastic elastomers are materials that combine the processing characteristics of thermoplastics with the physical properties of vulcanized rubbers. All thermoplastic elastomers are phase-separated systems in which one phase is hard and solid at room temperature while the other is elastomeric. The driving force for phase separation is the incompatibility of the hard and soft segments. The hard segments act as reinforcing fillers and multifunctional cross-links that are thermally reversible. It has been shown that the mechanical properties and morphology of these materials are significantly influenced by the microphase separation of the hard segments and the degree of order and cohesion that is found in the hard-phase microdomains.[1,2] There are at least four different types of interaction among hard segments that can act as a driving force for phase separation and hard-domain aggregation: van der Waals bonding in styrene–butadiene–styrene block copolymers,[3] hydrogen bonding in thermoplastic polyurethane elastomers,[4–6] crystallization of the polyester segments in poly(ether ester) thermoplastic elastomers,[7–9] and ionic interactions in some ionomers.[10] However, little attention has been given to the potential for coordination interactions between hard segments and the subsequent influence on the morphology and mechanical properties of thermoplastic elastomers.

In recent years, experimental results have been published on polymer blends based on coordination chemistry.[11–17] In 1978, Meyer and Pineri[11] found complexation in a terpolymer of butadiene, styrene, and poly(4-vinylpyridine). Using a number of techniques, they obtained evidence for three types of iron complexes. Agarwal et al.[12] described the preparation, rheology, and mechanical properties of polymer blends composed of sulfonated ethylene–propylene–diene elastomers (S-EPDM) and styrene 4-vinylpyridine copolymers (SVP) neutralized with transition metals. It was found that the rheological

* Permanent address: Department of Chemistry, Nanjing University, Nanjing, People's Republic of China.

† To whom correspondence should be addressed at College of Engineering, University of Delaware, Newark, DE 19716.

Journal of Applied Polymer Science, Vol. 51, 365–374 (1994)
 CCC 0021-8995/94/020365-10

and mechanical properties were strongly influenced by coordination between the transition-metal counterions of S-EPDM and the lone-pair electrons on the nitrogen of the vinylpyridine copolymer; nontransition-metal counterions, such as sodium and magnesium, did not coordinate strongly with pyridine. Lu and Weiss[13] studied the solution behavior of sulfonated polystyrene and poly(styrene-*co*-4-vinylpyridine). Although transition metals formed the strongest coordination, both alkali and alkaline earth metals also exhibited some interaction in solution. A schematic of the intermolecular complex was proposed, in which the cation is solvated to varying degrees by different solvents. They also suggested that two mechanisms for complexation are possible: one for blends with transition metals and one for blends containing nontransition metals. Several metal-containing poly(4-vinylpyridine) (P4VP) blends have been investigated in the solid state by Belfiore and co-workers.[14,15] Their results showed maxima in plots of glass-transition temperature vs. composition for several blends of metal acetates with P4VP. In a blend of zinc acetate and P4VP, the maximum enhancement in T_g was seen to be 20°C, at a composition of 16 mol % zinc acetate. However, the maximum enhancement of T_g in blends of nickel acetate with P4VP was about 100°C, with a metal/pyridine molar ratio of approximately 1 : 2. These results suggested that metal–ligand coordination could act as a driving force for phase separation and hard-domain cohesion in a thermoplastic elastomer that contained ligands in the hard segments.

In the present study, a new type of polyurethane was synthesized based on poly(tetramethylene glycol) (MW = 1000), 4,4′-diphenylmethylene diisocyanate (MDI), and *N,N*-bis(2-hydroxyethyl) isonicotinamide (BIN). This polyurethane contains pendant pyridine groups in the hard segment. The effects of coordination between the pyridine group and different metal acetate salts on phase separation and hard-domain aggregation were investigated. It was expected that this kind of interaction would provide a new type of driving force for phase separation and hard-domain cohesion in multiblock copolymers.

EXPERIMENTAL

Synthesis and Sample Preparation

The polyurethanes were synthesized using a two-step addition reaction. The polymers were based on 2/1/1 and 3/2/1 molar ratios of methylene diphenyldiisocyanate (MDI), *N,N*-bis(2-hydroxyethyl)isonicotinamide (BIN), and poly(tetramethylene glycol) (PTMO, MW = 1000). MDI (Polysciences) was melted and pressure-filtered at 60°C to separate the monomer from the dimers. *N,N*-Dimethylacetamide (DMAc) (anhydrous, 99+ %, Aldrich) and stannous octoate (catalyst T-9, Air Products) were used as received. The PTMO/DMAc solution, containing 0.15 wt % (based on all reactants) stannous octoate catalyst, was slowly added to the stirred MDI/DMAc solution at 60–65°C under a dry argon purge. After 1 h, the reactants were cooled to 55°C, and the chain extender (25% BIN in DMAc solution) was then added dropwise to the stirred prepolymer solution. Chain extension required 2 h at 60°C followed by 4 h at 75–80°C. The polymer was precipitated in hot distilled water, washed with methyl alcohol, and then dried in a vacuum oven at 65–70°C for a minimum of 2 days. The synthetic route is briefly outlined in Scheme 1.

Sample nomenclature, molecular weight from GPC, and elemental analysis data are shown in Table I. BIN–PU-35 represents the polyurethane chain-extended by BIN that contains 35 wt % MDI.

Blends of BIN–PU with metal acetates were prepared by dissolving the precursor polymer in dimethylformamide (DMF) (10 wt %), then mixing with a stoichiometric amount of the appropriate metal acetate dissolved in DMF at 50°C. The molar ratio of pyridine nitrogens to acetate groups was 1/1 for all blends. $Zn(OAc)_2 \cdot 2H_2O$, $Cu(OAc)_2 \cdot H_2O$, and $Ni(OAc)_2 \cdot 4H_2O$ (Aldrich) were used as received. The solutions were poured into Teflon-casting dishes and the solvent was evaporated in an air oven at 60°C for 24 h, after which the films were vacuum dried at 60°C for 48 h. Sample nomenclature and composition are shown in Table II.

Characterization Methods

The ^{13}C nuclear magnetic resonance (NMR) spectrum of BIN–PU-35 was recorded in DMSO by a GEMINI-300 NMR apparatus at 25°C. Pulse widths were 11.5 μs, with 4 s pulse delays. Standard proton decoupling was employed.

Gel permeation chromatography (GPC) was performed on a Waters Associates Model 501 equipped with ultraviolet (UV) and refractive index (RI) detectors, using *N,N*-dimethylacetamide (DMAc) with 0.2% lithium nitrate as the mobile phase. The measurements were carried out on 0.1 wt % polymer solution samples at 50°C using a flow rate of 0.5

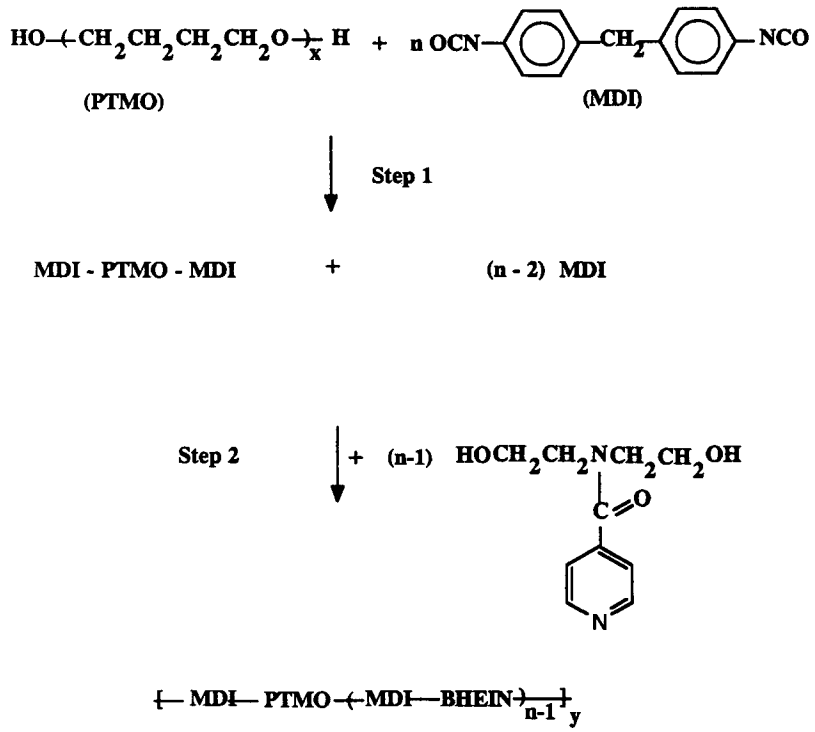

Scheme 1 Synthesis of BIN-extended polyurethane.

mL/min. The column was calibrated with polystyrene standards.

Uniaxial stress–strain data were obtained on an Instron Model TM using a crosshead speed of 0.5 in./min. The Instron was interfaced to a Gateway 386 personal computer that allowed automatic data collection. Samples were cut with an ASTM D1708 die. All stress–strain data are reported as engineering stress and are the average results of three tests. Standard deviations of Young's modulus and ultimate properties for all samples were within 20% of the average values.

Differential scanning calorimetry (DSC) was carried out with a Perkin-Elmer DSC2-C interfaced to a Model 3600 data station, using standard TADS software. Temperature calibration was set by the melting points of mercury and indium, with the latter also serving as an enthalpy reference. A heating rate of 20°C/min under a helium purge was used on samples of 15 ± 3 mg. The data processing software allows automatic background substraction and normalization of the thermogram for the sample weight. The glass transition temperature (T_g) was determined in the following way: Two straight lines

Table I Composition, Molecular Weight, and Elemental Analysis of BIN-extended Polyurethanes

						Elemental Analysis	
Materials	Composition	$M_n \times 10^{-4}$	$M_w \times 10^{-4}$	M_w/M_n		Exp	Theory
BIN-PU-35	MDI/BIN/PTMO 3/2/1	2.62	6.12	2.34	C%	65.19	66.12
					H%	7.98	7.98
					N%	6.25	6.37
					O%	20.58	19.6
BIN-PU-29	MDI/BIN/PTMO 2/1/1	2.35	5.87	2.50	C%	65.55	65.88
					H%	7.95	8.64
					N%	4.82	4.90
					O%	21.68	20.56

Table II Sample Designations and Composition of Blends of BIN–PU and Metal Acetates

SampleDesignation	Composition (Wt %)		Molar Ratio of Pyridine to Metal
BIN-PU-29/Zn	Bin-PU-29	93.0%	1/1
	$Zn(OAc)_2 \cdot 2H_2O$	7.0%	
BIN-PU-29/Cu	BIN-PU-29	93.63%	1/1
	$Cu(OAc)_2 \cdot H_2O$	6.37%	
BIN-PU-29/Ni	BIN-PU-29	92.17%	1/1
	$Ni(OAc)_2 \cdot 4H_2O$	7.83%	
BIN-PU-35/Zn	BIN-PU-35	90.0%	1/1
	$Zn(OAc)_2 \cdot 2H_2O$	10.0%	
BIN-PU-35/Cu	BIN-PU-35	90.75%	1/1
	$Cu(OAc)_2 \cdot H_2O$	9.25%	
BIN-PU-35/Ni	BIN-PU-35	88.73%	1/1
	$Ni(OAc)_2 \cdot 4H_2O$	11.27%	

were drawn along the linear portion of the DSC curves above and below the T_g. A third line was drawn at the inflection point of the glass transition region. The T_g was taken as the average of the intersection points of the third line with the two other lines; the change in heat capacity at the T_g was determined from the two intersection points as well.

Dynamic mechanical thermal analysis (DMTA) data were obtained with a Rheometrics RSA II in the tension mode. Samples were cut from cast films

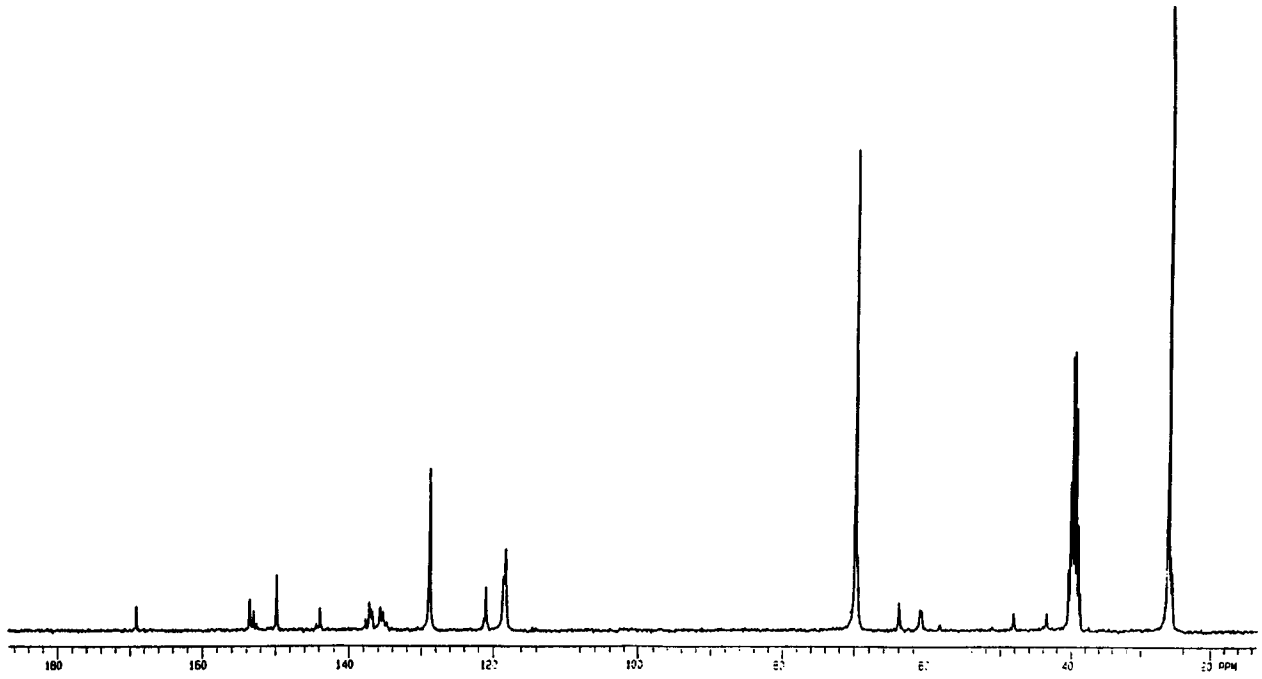

Figure 1 ^{13}C-NMR spectrum of BIN–PU-35 in DMSO.

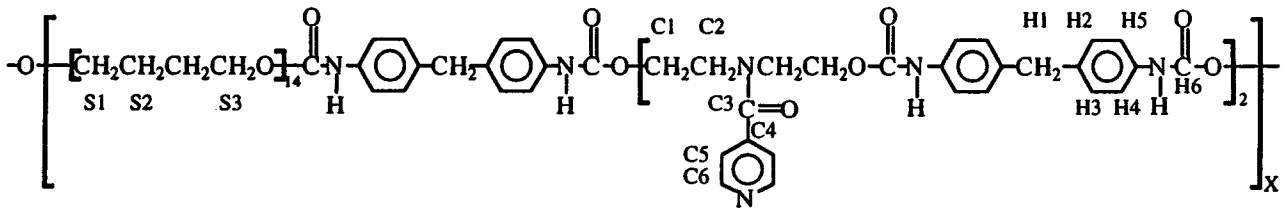

Scheme 2 Schematic of BIN-PU-35 and its peak assignments.

using an ASTM D1043 die. The approximate test dimensions were 23 × 6.3 × 1 mm. The temperature step was 3°C with 0.1 min soak time and the test frequency was 16 Hz over the temperature range of −150 to 250°C.

RESULTS AND DISCUSSION

NMR Results

The solution-state ^{13}C-NMR spectrum of BIN-PU-35 is shown in Figure 1; the peak assignments are presented in Scheme 2 and Table III. Assignments were made based on available literature values[18] and previous work done in this laboratory.[19] The ratio of the intensity of the MDI carbonyl peak to the intensity of the chain-extender carbonyl peak at 169 ppm is 3 : 1. Since each MDI contains two carbonyls and each chain extender contains one carbonyl, the ratio of MDI : BIN in the polymer corresponds precisely to the 3 : 2 stoichiometry of the reactants.

Two peaks, at 43 and 48 ppm, are assigned to the $\underline{C}H_2-N-$ carbon. The sum of the intensities of these two peaks is stoichiometrically proportional to the intensity of the chain-extender carbonyl peak, as well as being equal to the intensity of the chain-extender $\underline{C}H_2-O-$ peak. This suggests that these two peaks come from chemically equivalent carbons whose resonances are split due to conformational effects. The chemical shift of this carbon depends on its position with respect to the carbonyl group and pyridine ring, which are not rotating freely. According to the DSC trace, the pyridine group interacts weakly with the urethane protons. In addition, the carbonyl II orbital may preferentially align with the nitrogen lone electron pair, preventing rotation about the C(O)—N bond. Similar behavior was observed with the methyl protons of *N,N*-dimethylformamide (DMF) due to slow rotation about the C—N bond.[20] In another study, the chemical shifts of protons bonded to urea and urethane nitrogens changed when the materials were blended with LiCl; without LiCl, both types of protons had identical

Table III Chemical Shift Assignments for BIN-PU-35

Carbon Site	Carbon Label	Shift (ppm)
PTMO external CH_2 adjacent to urethane	S1	64
PTMO internal CH_2	S2	26
PTMO external CH_2	S3	70
MDI CH_2	H1	40
MDI internal quaternary ring	H2	137
MDI external quaternary ring	H5	135
MDI internal protonated ring	H3	129
MDI external protonated ring	H4	118
MDI urethane carbonyl	H6	153
Chain-extender external CH_2—O	C1	61
Chain-extender internal CH_2—N	C2	48, 43
Chain-extender carbonyl	C3	169
Pyridine quaternary aromatic	C4	144
Pyridine protonated aromatic	C5	121
Pyridine protonated aromatic adjacent to nitrogen	C6	150

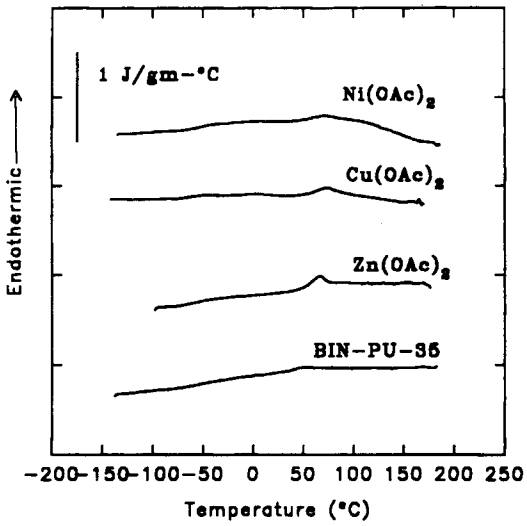

Figure 2 DSC results of BIN-PU-35 and its blends with different metal acetates.

chemical shifts.[21] It was suggested that preferential complexation led to the larger downfield shifts of the urea protons. These studies suggest that either interaction or slow molecular motion in a polymer can result in the kinds of peak splittings seen with BIN-PU-35.

DSC Results

DSC curves for BIN-PU-35, BIN-PU-29, and their blends with different metal acetates are shown in Figures 2 and 3, respectively. Thermal analysis and thermal transition results for the BIN-PU-35 and BIN-PU-29 series of materials are summarized in Table IV. The shift of soft-segment T_g to lower temperature as hard-segment content (MDI plus chain extender) changes from 42 to 54% indicate that the degree of phase separation increases with increasing hard-segment content. Comparing the DSC data of BIN-PU-35 and its blends with different metal acetates, it is clear that blending with metal acetates increases the phase separation between the hard and soft segments. Based on the T_g values of these blends, the degree of phase separation increases in the order BIN-PU-35 < BIN-PU-35/Zn < BIN-PU-35/Cu $\approx$ BIN-PU-35/Ni. These results can be explained in terms of the strength of the interaction between the pyridine group and the given metal acetate. A comparison of the DSC results from the BIN-PU-29 series shows that the T_g of metal acetate blends did not exhibit the same trend as in the BIN-PU-35 series. In the BIN-PU-29 series, the T_g of all the metal blends were within 1°C, which is within the experimental error of the DSC experiments. However, the T_g's of all the metal blends were slightly lower than that of the BIN-PU-29 precursor. Another difference between the BIN-PU-35 series and the BIN-PU-29 series is that the former showed an additional endotherm at around 60°C. This small endotherm may be interpreted as a short-range ordering of hard segments, which are longer in the BIN-PU-35 series than in the BIN-PU-29 series.

Dynamic Mechanical Thermal Analysis

The dynamic mechanical thermal analysis (DMTA) results for the BIN-PU polyurethanes and their blends with different metal acetates are presented in Figures 4–6. Glass-transition data are summarized in Table IV. The low-temperature transition (γ peak) and the T_g of the soft segment (β peak) were determined from their peak positions in the loss modulus (E'') curves.

From the DMTA curves of the two BIN-PU precursors, there is a 8°C difference in soft-segment T_g. This difference suggests that the phase separation is enhanced with increases in the length and percentage of the hard segment, which is consistent with the DSC data. The rubbery plateau modulus also increases significantly in magnitude with increasing hard-segment content. The rubbery plateau modulus of BIN-PU-35 is higher than that of BIN-PU-29 by almost two orders of magnitude. Thus,

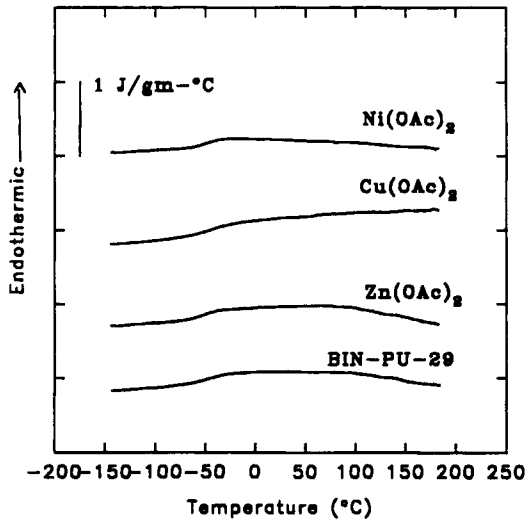

Figure 3 DSC results of BIN-PU-29 and its blends with different metal acetates.

Table IV Thermal Transition Data of BIN–PU-35, BIN–PU-29, and Their Blends with Different Metal Acetates

	DSC Results		DMTA Results		
Sample Code	T_g (°C)	Endotherm (°C)	γ (peak) (°C)	β (Peak) (°C)	Rubber Plateau (°C)
BIN–PU-29	−49	—	−137	−40	33–133
BIN–PU-29/Zn	−51	—	−137	−43	3–118
BIN–PU-29/Cu	−51	—	−134	−43	3–115
BIN–PU-29/Ni	−51	—	−136	−44	3–123
BIN–PU-35	−52	54	−136	−48	−17–100
BIN–PU-35/Zn	−54	67	−135	−50	−17–103
BIN–PU-35/Cu	−59	69	−135	−52	−19–111
BIN–PU-35/Ni	−58	69	−137	−54	−20–142

the morphology of these two series of materials may be substantially different. For BIN–PU-29, a more discontinuous hard domain dispersed in a soft-segment matrix is expected, whereas an interconnected hard domain is likely for BIN–PU-35 since the weight percentage of hard segment is 54%.

Figure 5 shows the DMTA curves of BIN–PU-35 and its blends with different metal acetates. Both the degree of phase separation and the rubbery plateau increase with the addition of metal acetates and follow the order of BIN–PU-35/Ni > BIN–PU-35/Cu > BIN–PU-35/Zn > BIN–PU-35. This suggests that the metals interact with the pyridine groups in the hard segment and that the strength of this interaction depends on the coordination ability of the different metal ions. The interaction between pyridine and Ni is the strongest among the three. Again, the results are in agreement with the DSC data.

The DMTA curves for BIN–PU-29 and its blends with different metal acetates are given in Figure 6. The behavior of the BIN–PU-29 series is different from that of BIN–PU-35 series. In the BIN–PU-35 series, blending with metal acetates extends the rubbery region without dramatically changing the rubbery plateau modulus. However, in the BIN–PU-29 series, the length of the rubbery plateau regions remain relatively constant before and after blending

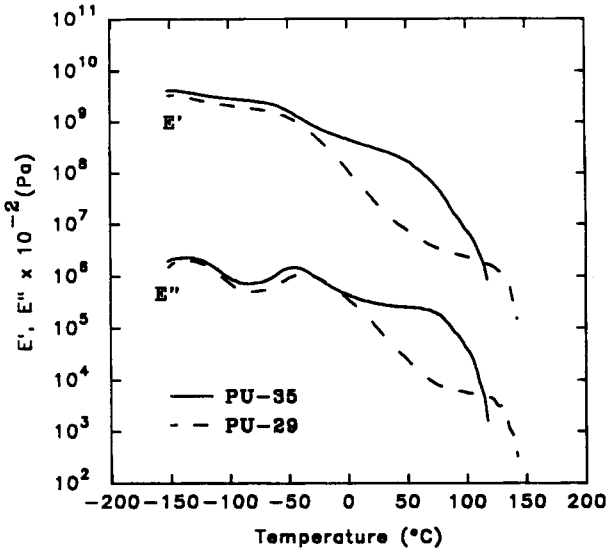

Figure 4 DMTA results of BIN–PU-35 and BIN–PU-29.

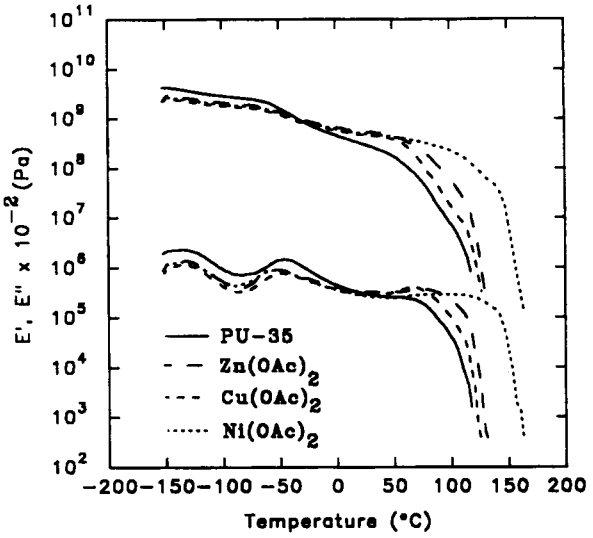

Figure 5 DMTA results of BIN–PU-35 and its blends with different metal acetates.

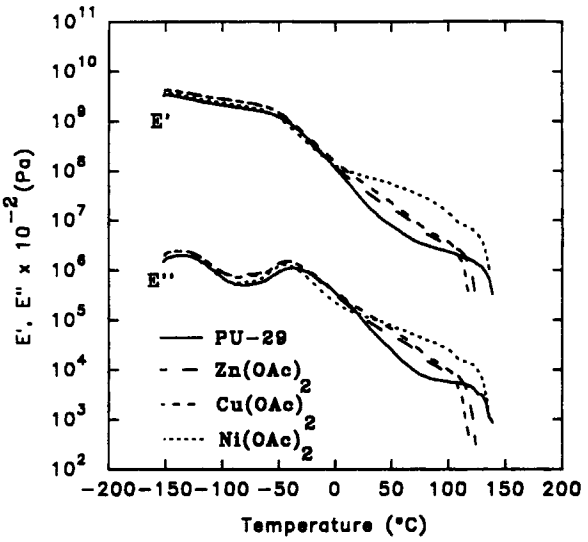

Figure 6 DMTA results of BIN–PU-29 and its blends with different metal acetates.

with metal acetates, while the rubbery plateau modulus changes by almost one order of magnitude. This phenomenon might be explained by the proposed difference in the precursor polymer morphologies. The interaction of metal ions with pyridine ligands can dramatically enhance the hard-domain cohesion. For an interconnected hard-domain morphology, this interaction mainly improves the strength of the hard-segment microphase whose softening point results in a downturn in modulus. However, for a dispersed hard-domain morphology, the number of physical cross-links may be changed. Stronger metal–ligand interactions may result in smaller and more dispersed hard domains and a subsequent increase in the effective number of cross-links.

Tensile Properties

The stress–strain curves for BIN-extended polyurethanes and their blends with different metal acetates are shown in Figures 7 and 8. It is apparent from the tensile-property data summarized in Table V that the Young's moduli of the BIN–PU-29 blends are two to four times higher than that of the precursor polymer. However, for the BIN–PU-35 series, the moduli of the blends are 10–35 times higher than that of the precursor material. For both the BIN–PU-29 and BIN–PU-35 series, the Young's moduli increase in the order BIN–PU/Ni > BIN–PU/Cu > BIN–PU/Zn > BIN–PU. These experimental data provide further evidence that the metal acetates coordinate with the pyridine ligand in the hard segment and that the interaction between pyridine and Ni is the strongest one. The data also suggest that the morphologies of the two series are different. Increased hard-domain cohesion would be expected to increase the Young's modulus to a greater extent for materials with an interconnected hard-domain morphology. It is interesting to note that the precursor polymers show only slightly less phase separation than do the blends, yet they have dramati-

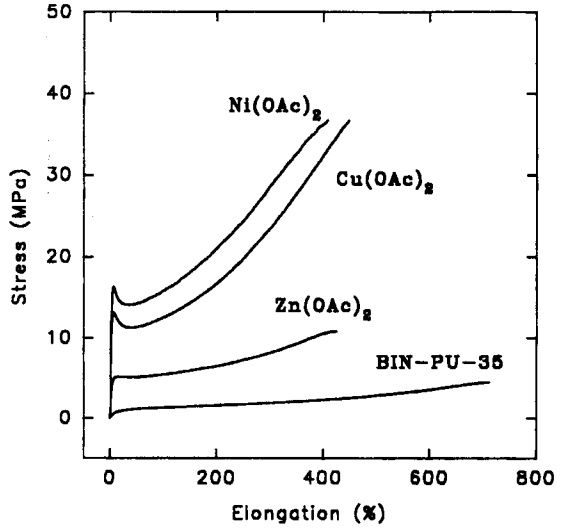

Figure 7 Stress–strain curves of BIN–PU-35 and its blends with different metal acetates.

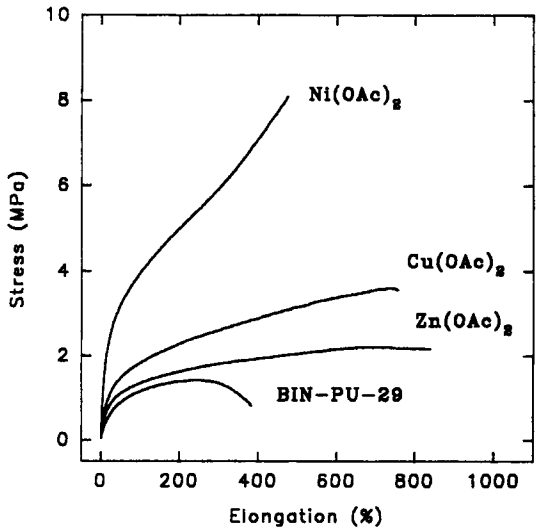

Figure 8 Stress–strain curves of BIN–PU-29 and its blends with different metal acetates.

Table V Tensile Properties of BIN–PU-35, BIN–PU-29, and Their Blends with Different Metal Acetates

Samples	Young's Modulus E_0 (MPa)	Elongation at Break (%)	Ultimate Stress (MPa)
BIN–PU-35	12	710	4.5
BIN–PU-35/Zn	110	430	11
BIN–PU-35/Cu	350	450	37
BIN–PU-35/Ni	450	410	37
BIN–PU-29	4.8	380	0.8
BIN–PU-29/Zn	7.3	840	2.2
BIN–PU-29/Cu	9.2	760	3.6
BIN–PU-29/Ni	20	480	8.1

cally lower strength. This suggests that hard-domain cohesion is more important to mechanical strength than is the degree of phase separation.

From a comparison of the tensile-testing data for the BIN–PU-29 and BIN–PU-35 series, it is apparent that blending with metal acetates improves the stress-at-break for both series. However, there are some differences between the two series of blends. First, for the BIN–PU-29 blends, the elongation at break decreases as the metal ion changes from Zn to Cu(II), then to Ni. However, the elongation-at-break for BIN–PU-35 blends does not show a significant difference. Furthermore, there is no yielding in the BIN–PU-29 series, whereas yield points are observed in the case of BIN–PU-35 blends with nickel and copper acetates. These results can also be attributed to the proposed morphologies. For the BIN–PU-29 series, blending with different metal acetates is believed to increase the number of cross-links and, thus, cause the elongation-at-break to decrease. The yield points that appear in the BIN–PU-35 blends can be explained by their interconnected hard-domain morphology.

SUMMARY AND CONCLUSION

A new type of pyridine-containing polyurethane was synthesized based on MDI/BIN/PTMO-1000, with stoichiometries of 3/2/1 and 2/1/1. These polyurethanes show a mechanism for phase separation other than van der Waals, hydrogen bonding, ionic interaction, and crystallization commonly found in multiphase block copolymers. The mechanism depends on coordination between an electron donor, in this case pyridine, and transition-metal ions. The interaction was achieved by blending pyridine-containing polyurethanes with metal acetates. Results from DSC, DMTA, and tensile testing show that interactions exist between the pendant pyridine group and metal ions in the hard domains. The coordination strength with the pyridine group is a function of the metal ion and follows the order BIN–PU/Ni or BIN–PU/Cu > BIN–PU/Zn. Observations of a decrease of the soft-segment T_g in DSC, extension of the rubbery plateau region in DMTA, and increases of the Young's modulus and stress at break in tensile testing all suggest that pyridine–metal coordination results in greater phase separation and increased hard-domain cohesion. Two different morphologies are proposed for the BIN–PU-29 and BIN–PU-35 series to explain differences in the DMTA and tensile data. Polymers in the BIN–PU-35 series are believed to have an interconnected hard-domain morphology, whereas those in the BIN–PU-29 series have a morphology of dispersed hard domains in a soft-segment matrix. For the interconnected hard-domain morphology, interactions between metal ions and pyridine groups mainly improve the strength of the interconnected microphase material. For a dispersed hard-domain morphology, the interactions may change the effective number of physical cross-links. These morphological differences can account for the changes in rubbery plateau modulus observed in DMTA and in elongation at break and the occurrence of a yield point observed in tensile testing.

Support for this work was provided by NSF grant DMR-9016959. E. M. O. and R. J. G. gratefully acknowledge the support of the Department of Defense through the National Defense Science and Engineering Graduate Fellowships.

REFERENCES

1. S. L. Cooper and A. V. Tobolsky, *J. Appl. Polym. Sci.*, **10,** 1837 (1966).
2. G. M. Estes, R. W. Seymour, and S. L. Cooper, *Macromolecules,* **4,** 452 (1971).
3. G. M. Estes, S. L. Cooper, and A. V. Tobolsky, *J. Macromol. Sci.-Rev. Macromol. Chem.*, **C4**(2), 313 (1970).
4. R. W. Seymour, G. M. Estes, and S. L. Cooper, *Macromolecules,* **3,** 579 (1970).
5. P. E. Gibson, M. A. Vallance, and S. L. Cooper, in *Developments in Block Copolymers-1,* I. Goodman, Ed., Applied Science, New York, 1982.
6. G. Oertel, Ed., *Polyurethane Handbook,* Hanser, New York, 1985.
7. J. C. Stevenson, and S. L. Cooper, *Macromolecules,* **21,** 1309 (1988).
8. R. J. Cella, *J. Polym. Sci. C,* **42,** 727 (1973).
9. L. Zhu, G. Wegner, and U. Bandara, *Makromol. Chem.*, **182,** 3639 (1981).
10. A. Eisenberg and M. King, *Ion-Containing Polymers,* Academic Press, New York, 1977.
11. C. T. Meyer and M. Pineri, *J. Poly. Sci. Polym. Phys.*, **16,** 569 (1978).
12. P. K. Agarwal, I. Duvdevani, and D. G. Peiffer, *J. Poly. Sci. Polym. Phys.*, **25,** 839 (1987).
13. X. Lu and R. A. Weiss, *Macromolecules,* **24,** 5763 (1991).
14. L. A. Belfiore, A. T. N. Pires, Y. Wang, H. Graham, and Eiji Ueda, *Macromolecules,* **25,** 1411 (1992).
15. L. A. Belfiore, H. Graham, and E. Ueda, *Macromolecules,* **25,** 2935 (1992).
16. N. H. Agnew, *J. Polym. Sci. Poly. Chem. Ed.,* **14,** 2819 (1976).
17. D. G. Peiffer, I. Duvdevani, and P. K. Agarwal, *J. Polym. Sci. Polym. Lett. Ed.,* **21,** 581 (1986).
18. F. Toda, Ed., *Handbook of ^{13}C NMR Spectra,* Sanyo, Tokyo, 1981.
19. D. T. Okamoto, S. L. Cooper, and T. W. Root, *Macromolecules,* **25,** 1068 (1992).
20. J. I. Kaplan and G. Fraenkel, *NMR of Chemically Exchanging Systems,* Academic Press, New York, 1980.
21. Y. Chokki, *Makromol. Chem.*, **175,** 3425 (1974).

Received December 14, 1992
Accepted June 22, 1993